Research Article

Fayez M. Saleh, Hattan Gattan, Bassam M. Al-Ahmadi, Abdullah F. Shater, Zuhair M. Mohammedsaleh, Awatif M. E. Omran, Rasha Jame, Noha Omer, Yahya S. Al-Awthan, Elham M. Alhathli, Hamza S. Al-Shehri, Syed Khalid Mustafa, Adel D. Althaqafy, Hatem A. Al-Aoh, and Chellasamy Panneerselvam*

Characterization of silver sulfide nanoparticles from actinobacterial strain (M10A62) and its toxicity against lepidopteran and dipterans insect species

https://doi.org/10.1515/gps-2023-0147
received August 7, 2023; accepted November 15, 2023

Abstract: In this research, cell-free extracts from magnesite mine-isolated actinobacterial strain (M10A62) were used to produce silver sulfide nanoparticles (Ag_2SNPs). *Streptomyces minutiscleroticus* JX905302, actinobacteria capable of producing Ag_2SNPs, was used to synthesize Ag_2NPs. The UV–vis range was used to confirm the biosynthesized Ag_2NPs; Fourier transform infrared spectroscopy (FT-IR), atomic force microscopy (AFM), transmission electron microscopy (TEM), X-ray diffraction (XRD), energy-dispersive X-ray spectroscopy (EDAX), and dynamic light scattering analysis were employed to characterize them further. Surface resonance plasma (SRP) for Ag_2SNPs was obtained at 355 nm using UV–visible spectroscopy; FT-IR detected bimolecular and eventually microbial-reduced Ag_2SNPs from *S. minutiscleroticus* culture extract. Furthermore, AFM and TEM analysis confirms that the synthesized Ag_2SNPs were spherical in shape. Dynamic light scattering revealed a negatively charged Ag_2NPs surface with a diameter of 10 nm. The XRD spectrum showed the crystalline nature of the obtained particles. EDAX revealed a pure crystalline nature, and a significant silver particle signal confirms the presence of metallic silver and sulfide nanoparticles together with the signals of Cu and C atoms. After 40 and 48 h of treatment at 150–200 $\mu g \cdot ml^{-1}$, Ag_2SNPs produced the highest mortality in *Spodoptera litura*, *H. armigera, Aedes aegypti*, and *Culex quinquefasciatus* larvae. Hence, the biosynthesized Ag_2SNPs may be useful for potential pest control in integrated pest management and vector control program as a safer, cost-effective, selective, and environmentally friendly approaches.

Keywords: actinobacteria, silver sulfide nanoparticles, biosynthesis, insecticidal activity

*** Corresponding author: Chellasamy Panneerselvam**, Department of Biology, Faculty of Science, University of Tabuk, Tabuk 71491, Saudi Arabia, e-mail: cpselva@ymail.com
Fayez M. Saleh: Department of Medical Microbiology, Faculty of Medicine, University of Tabuk, Tabuk 71491, Saudi Arabia
Hattan Gattan: Department of Medical Laboratory Sciences, Faculty of Applied Medical Sciences, King Abdulaziz University, Jeddah, Saudi Arabia; Special Infectious Agents Unit, King Fahad Medical Research Center, Jeddah, Saudi Arabia
Bassam M. Al-Ahmadi: Department of Biology, Faculty of Science, Taibah University, Taibah, Saudi Arabia
Abdullah F. Shater, Zuhair M. Mohammedsaleh: Department of Medical Laboratory Technology, Faculty of Applied Medical Sciences, University of Tabuk, Tabuk 71491, Saudi Arabia
Awatif M. E. Omran: Department of Biochemistry, Faculty of Science, University of Tabuk, Tabuk 71491, Saudi Arabia
Rasha Jame, Noha Omer, Syed Khalid Mustafa, Adel D. Althaqafy, Hatem A. Al-Aoh: Department of Chemistry, Faculty of Science, University of Tabuk, Tabuk 71491, Saudi Arabia
Yahya S. Al-Awthan: Department of Biology, Faculty of Science, University of Tabuk, Tabuk 71491, Saudi Arabia
Elham M. Alhathli: Department of Nursing, Faculty of Applied Medical Sciences, Taif University, Taif, Saudi Arabia
Hamza S. Al-Shehri: Chemistry Division, King Khalid Military Academy, SANG 11495, Riyadh, Saudi Arabia

1 Introduction

The focus of nanoparticles is on the development of nanotechnology in several fields, such as material science, medical, agricultural, and environmental remediation [1,2]. Nanoparticles (NPs) have increased catalytic, mechanical, optical, and magnetic properties due to their high surface

area-to-volume ratio [3]. Among various nanomaterials (gold, silver, copper, iron, aluminum, cobalt, titanium, and zinc), silver NPs have offered novel designs of NPs (1–100 nm) that were used in various pest management programs [4,5]. Recently, silver sulfide NPs (Ag_2SNPs) synthesized from green plants and microbial origin have gained an important place in nanofabrication with a wide range of applications, including anticancer, anti-inflammatory, anthelmintic and wastewater treatment, and antimicrobial properties [6,7].

The phylum Actinomycetota is primarily composed of gram-positive bacteria with a high nitrogenous base content. By acting as a reducing agent, the metabolites secreted by these bacteria can promote the fusion of NPs [8]. For instance, AgNPs synthesized by *Nocardiopsis* sp. MBRC-1 (marine antimicrobial strain) showed potent antimicrobial and cytotoxic properties [9]. Similar results were obtained when *Streptomyces xinghaiensis* OF1-derived AgNPs were tested against pathogenic bacteria and yeast [10]. Due to their metal nature, AgNPs must be suited for a biological system to reduce their cytotoxic effect and the ways in which they interact and connect with biological cells [11].

The common cutworm and cotton bollworm (*Spodoptera litura* and *H. armigera*) are well-known lepidopteran agricultural pests that almost occupy entire agricultural crops due to their polyphagous nature and are responsible for major crop damage [12]. Besides crop pests, mosquitoes, *Aedes aegypti* and *Culex quinquefasciatus*, served as a vector for spreading many deadly diseases worldwide [13]. Since their outbreak as a pest, the persistent use of chemical insecticides to combat these insect pests may lead to the development of resistance against them through various resistance mechanisms [14]. Apart from resistance, chemical insecticide residues may harm the environment, humans, and other non-target organisms [15]. Therefore, alternatives to chemical pesticides for insect pest management must be investigated. Nanotechnology has provided a different strategy for the pest control program to overcome pesticide resistance [16].

Numerous lines of research have demonstrated the antimicrobial characteristics of AgNPs; however, the insecticidal properties of Ag_2SNPs produced through biological synthesis have not been studied properly [17,18]. Comparably, various biomedical applications and mosquito larvicidal activities of selenium NPs synthesized from the M10A62 strain [19,20]. Hence, the present study investigated the biosynthesis of Ag_2SNPs and its possible application in pest control using the *Streptomyces minutiscleroticus* actinobacterial strain (M10A62) isolated from a magnesite mine soil sample.

2 Materials and methods

2.1 Actinobacterial strain

S. minutiscleroticus M10A62 (GenBank Accession Number: JX905302) actinobacterial strain was isolated from a magnesite mine soil sample from Salem district, Tamil Nadu, India. This strain was isolated on casein starch agar (CSA) medium with the supplement of ampicillin (15 $\mu g \cdot ml^{-1}$) and fluconazole (20 $\mu g \cdot ml^{-1}$) to inhibit undesirable microorganism development and purified on ISP-2 (International Streptomyces Project 2) medium [21]. The phenotypic characterization was done by TEM analysis to confirm the presence of aerial and substrate mycelium; further, 16s rDNA sequencing was used to confirm the strain of *Streptomyces* sp. [19].

2.2 Biosynthesis of Ag_2SNPs

The Ag_2SNPs were synthesized by using a shaking incubator. For 5 days at 250 rpm, the *S. minutiscleroticus* M10A62 strain was transferred to a 250 ml conical flask filled with 100 ml of yeast and malt extract broth and placed in a shaking incubator. Further, the biomass and cell fluids were separated by centrifugation, which ran for 30 min at 4°C and 6,000 rpm. 5 g of fresh, wet biomass was added to a 100 ml aqueous solution containing 1 mM $AgNO_3$ (silver nitrate) and $Na_2S{\cdot}9H_2O$ (sodium sulfide nonahydrate), rinsed three times with sterile distilled water, and mixed (HiMedia). After 48 h of consistent shaking at 250 rpm, at room temperature, the entire mixture was centrifuged for 30 min at 10,000 rpm to obtain a cell extract that was used in subsequent research.

2.3 Characterization of Ag_2SNPs

2.3.1 UV–visible spectral analysis

The visual color shift of the media from white to black served as a preliminary confirmation of the biosynthesis of Ag_2SNPs [28]. Afterwards, the mixture was centrifuged at 5,000 rpm for 15 min to separate the nanoparticles from the liquid. The reduction of nanoparticles was observed in a UV–vis spectrophotometer (Cyber Lab dual-beam spectrophotometer) at the wavelength of 200–700 nm by using 2 ml of aqueous solution at 1 nm resolution [22].

2.3.2 Fourier transform infrared spectroscopy (FT-IR) analysis

FT-IR was used to examine the nanoparticles containing allied functional groups (free amines, amides, or cysteine residues of protein) using the FT-IR model EXI. The lowest amount of dried powder sample was ground with 100 mg of potassium bromide of FT-IR quality before being formed into a pellet [23]. The compressed sample was held in the sample holder, and infrared spectra with a resolution of 4 cm^{-1} in the wavelength range of 400–4,000 cm^{-1} were collected. By contrasting functional peaks with already-existing peaks, the resulting nanoparticle spectrum was identified.

2.3.3 Atomic force microscopic (AFM) analysis

AFM analysis was carried out to monitor surface images of Ag_2SNPs by using Nanosurf-AFM. The samples were prepared by mixing nanoparticles with methanol, and a drop of the mixture was coated in a silicon slide and further evaporated to form a thin film. Finally, a thin film (1 cm × 1 cm) containing the sample was observed using AFM [24].

2.3.4 X-ray diffraction (XRD) analysis

An XRD (SHIMADZU XRD 6000) was used to analyze the purity and phase formation in Ag_2SNPs by using a 40 kV voltage and 30 mA current. The nanoparticle samples were centrifuged at 5,000 rpm for 20 min to ensure purity and redispersed in 10 ml of sterile deionized water. Then, the samples were freeze-dried, powdered, and used for structural characterization. The lucid nature of the nanoparticles was identified by comparing the XRD peaks with the Joint Committee on Powder Diffraction Standards (JCPDS) pattern [25].

2.3.5 Transmission electron microscopic (TEM) analysis

The morphological structure of the Ag_2SNPs was determined by the TEM model (HITACHI H-600). The silver sulfide sample was prepared by mixing nanoparticles with methanol and ground well. Further, the samples were dehydrated with acetone and infiltrated. Then, the drop of the sample solution was coated in a silicon slide and evaporated to form a thin film, and 1% osmium tetraoxide was poured over the slide, which acts as a post-fixative agent. By using TEM analysis at 80 kV, the size and form of the nanoparticles in the carbon-coated copper grid were determined [26].

2.3.6 AFM analysis

AFM was used to analyze the size of the synthesized Ag_2SNPs with selected area electron diffraction [27]. The samples were diluted in distilled water in a 1:9 ratio for AFM analysis. Then, two drops of the dilution were placed in a sample holder and allowed to air dry.

2.3.7 Dynamic light scattering (DLS) analysis

To determine the nanoparticle size dispersion, DLS was used. By injecting 2 ml of deionized water into the interior flow cell, the remaining particles that were present in the flow cell were removed. In order to determine a baseline scattering intensity, the light scattering measurements were logged for 2 min. A 1 ml syringe with 0.8 ml of nanoparticle solution was streaming into the flow cell at the end of the baseline intensity setup. To investigate the scattering intensity within the detector limit, only 0.7 ml of the 0.8 ml solution was pumped into the flow cell. The flow rate was halted once the 0.7 ml of solution had entered the flow cell, and the light scattering measurement was taken for 25 min. Subsequently, sterilized deionized water was used to flush out the nanoparticle's solution [28].

2.3.8 EDAX analysis

The percentage of the elemental composition of the nanoparticles was determined by EDAX studies by using Bruker AXS Inc., USA, Quantax-200 micro-analysis system coupled with TEM [29].

2.4 Insecticidal activity of Ag_2SNPs on lepidopteran insects

The toxicity of biosynthesized Ag_2SNPs was investigated on two important lepidopteran insects using the leaf dip method [30]. The *H. armigera* and *S. litura* (Accession no. NBAII-MP-NOC-01) egg mass was purchased from the National Bureau of Agricultural Insect Resources live insect repository (NBAIR), Bangalore, Karnataka, India. The first instar larvae hatched from each culture were maintained in the laboratory on castor leaves (25 ± 1°C, 70 ± 5% RH, and 12:12 h light: dark) without exposure to any insecticide. Fresh, clean, and young castor leaves were soaked in different concentrations of Ag_2SNPs (10, 50, 100, 150, and 200 $\mu g \cdot ml^{-1}$) for 20 s and left for a few minutes until getting dry; the control received water only.

Approximately 25 early third instar *H. armigera* and *S. litura* larvae were released in Ag_2SNPs dipped and control leaves. Three replications were maintained for each concentration. After 14, 24, 36, 40, and 48 h of treatment, the larval mortality was determined.

2.5 Insecticidal activity of Ag_2SNPs on dipterans insects

The insecticidal activity of Ag_2SNPs was evaluated on two dipterans insects as per the method of Muthusamy and Shivakumar [31]. The *Ae. aegypti* and *Cx. quinquefasciatus* were collected in the form of egg mass and egg raft from the Institute of Vector Control and Zoonoses (IVCZ, Hosur, Tamil Nadu, India). The eggs were brought into the laboratory and cultured under controlled conditions (25 ± 1°C, 70 ± 5% RH, and 12:12 h light: dark) on fresh tap water containing trays covered with mosquito net cloth. During the culture period, dog biscuits were provided as larval food. The newly hatched early third instar mosquito larvae were used for the insecticidal efficacy of Ag_2SNPs. Serial concentrations of Ag_2SNPs were prepared (as mentioned above) in a 250 ml paper cup containing distilled water. There were three replicates for each dose, and 25 larval (uniform-sized) were released in each paper cups; the control received only water. The larval mortality was assessed at 7, 14, 24, 36, 40, and 48 h of post treatment.

3 Results and discussion

The Actinobacteria are a significant bacterial group that is present in both terrestrial and aquatic settings. It has economic importance as a source of many antibiotics and the decomposing ability of many organic matters [32]. The present study revealed that five bacterial isolates with vegetative mycelium development on selective media were isolated. However, based on the quantitative analysis of metal-producing ability, actinomycete isolate *S. minutiscleroticus* M10A62 strain was used in this research to produce Ag_2SNPs in the fight against target insect pests.

Figure 1 illustrates the morphological characteristics of the M10A62 strain, and the texture and color of white aerial mycelium are depicted in Figure 1a. The SEM image (Figure 1b) shows the morphology of spores with recti flexible (RF) arrangement of smooth surface. After being identified as a potential source of AgNPs, physicochemical characteristics such as temperature, pH, and various reaction combinations were optimized [33]. The conversion of $AgNO_3$ and $Na_2S{\cdot}9H_2O$ into Ag_2SNPs was validated during M10A62 strain incubation by color changes to a brown, yellow, indicating the production of Ag_2SNPs (Figure 2a and b), is well in accord with the reports of Ramya et al. [20].

The UV–vis spectrum data revealed the confirmation of Ag_2SNP production, and the surface plasma resonance (SPR) phenomenon was responsible for the color shift [34]. The absorption maxima of synthesized Ag_2SNPs were obtained at 355 nm (Figure 3). The FT-IR measurement was used primarily to identify the possible biomolecules that are acting as reducing agents in Ag_2SNP synthesis by actinobacterial culture filtrate (Figure 4). The FT-IR spectra of Ag_2SNPs showed various bands at different wave numbers with respective functional groups (Table 1). The observation for Ag_2SNPs indicates that the protein binds to nanoparticles by means of free amines, amides or cysteine residues of protein bind to the negatively charged groups of enzymes present in the cell wall of actinobacterial mycelium through the electrostatic interaction [35,20]. Further, AFM

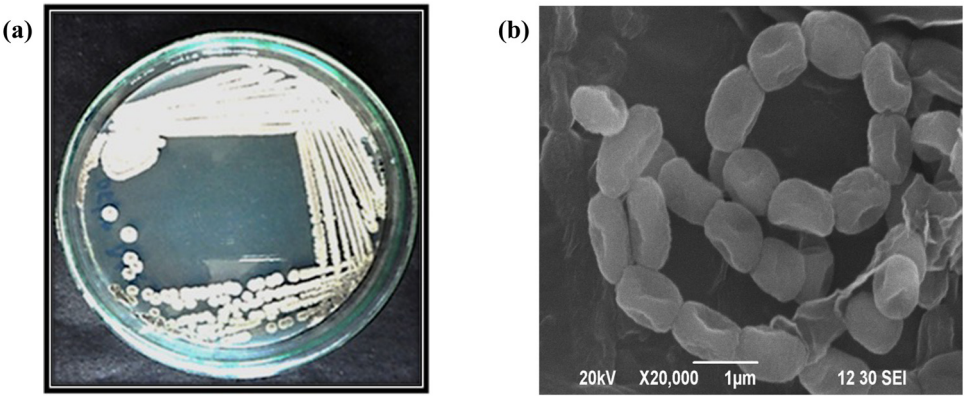

Figure 1: Morphological characteristics of *S. minutiscleroticus* M10A62 (a); (b) SEM analysis of strain M10A62.

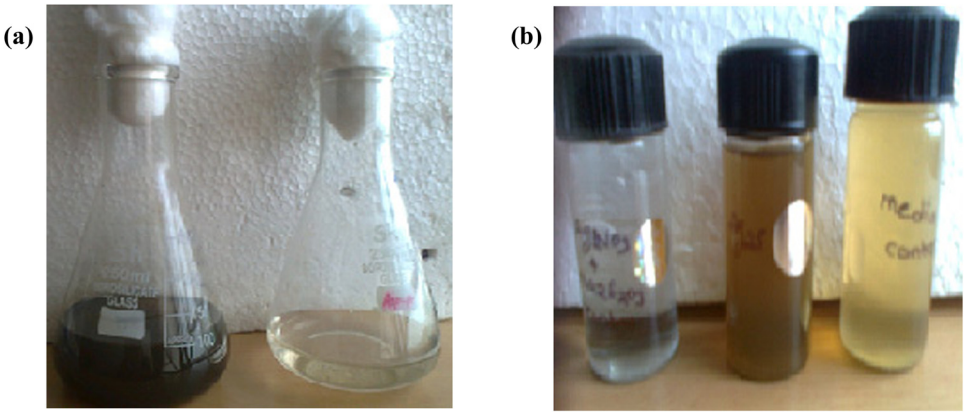

Figure 2: Production of Ag_2SNPs by M10A62 strain (a and b).

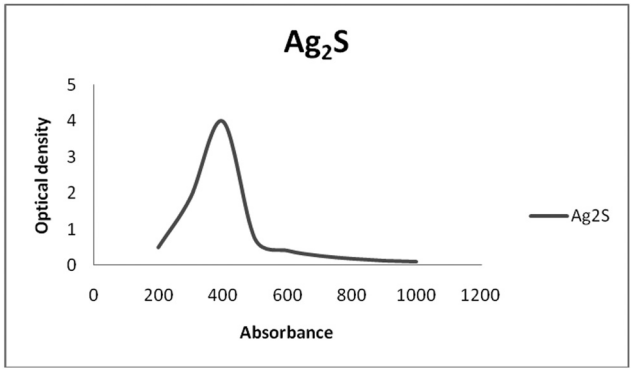

Figure 3: UV–visible spectra of *S. minutiscleroticus* derived Ag_2SNPs.

analysis shows that the synthesized Ag_2SNPs were mostly spherical in shape with an average size ranging from 0.5 to 5 µm, respectively (Figure 5).

The TEM pictures revealed that the actinobacterial strain M10A62 produced well-disseminated nanoparticles that were attached to capping protein molecules. The morphology and size of the Ag_2SNPs were 50–85 nm in size with spherical in shape (Figure 6). TEM analysis results were well matched with Ramya et al. [19], who studied the biological properties of actinobacterial-synthesized selenium nanoparticles. Figure 7 shows the XRD pattern of the Ag_2SNPs exhibited strong reflections at 2θ values of 46.25°, 44.12°, 32.23°, and 37.10° corresponding to the planes −111, 111, 112, and 120 (JCPDS card No. 14-0072). Comparably,

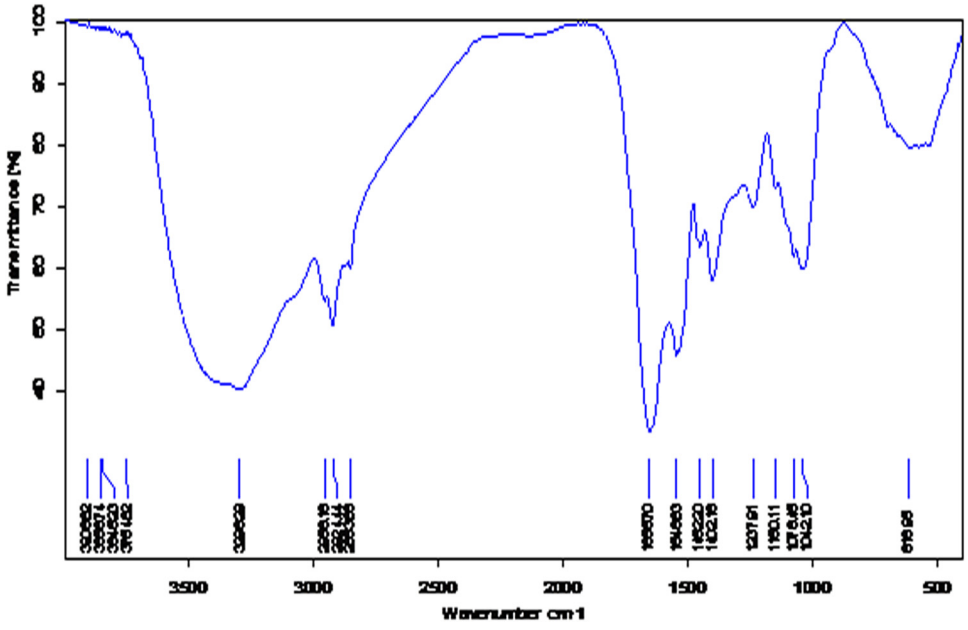

Figure 4: FT-IR spectrum of *S. minutiscleroticus* derived Ag_2SNPs.

Table 1: FT-IR peaks and their functional groups for Ag_2SNPs

S. No	Peaks (cm^{-1})	Functional groups
1	3,777	Strong sharp O–H stretching
2	3,471	Amide I
3	2,926	C–H stretching
4	2,139	Alkyene
5	1,776	C═O stretching
6	1,650	Amide II
7	1,597	Amide conjugated
8	1,356	Amide III
9	1,128	C–N stretching
10	1,019	C–O stretching
11	647	Residues of NO_3^-

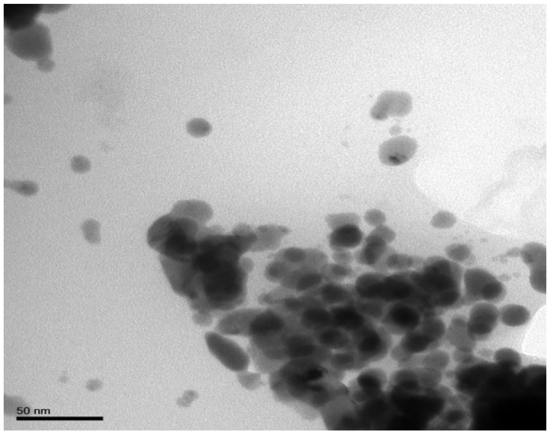

Figure 6: TEM image of *S. minutiscleroticus* derived Ag_2SNPs.

similar results from pomegranate peel extract and *Nicotiana tabacum* leaf extract derived XRD pattern were documented [36,37]. The dynamic light dispersion experiment revealed that Ag_2SNP particle size was about 10 nm (Figure 8). Figure 9 illustrates that the EDAX analysis of sulfide nanoparticles exhibited a strong signal at 3 keV due to SPR [10,38].

Numerous researchers have studied the toxic effect of nanoparticles on pathogenic bacteria and other pathogens of animals [39–41]. There have been relatively few investigations on the biocidal effect of biosynthesized nanoparticles [42,43]. However, no reports were evidenced in Ag_2SNPs against insects as insecticidal compounds. The biosynthesized Ag_2SNPs from the M10A62 strain were shown to have a high mortality rate on *S. litura* and *H. armigera* at 150 and 200 $g{\cdot}ml^{-1}$ after 40 and 48 h post-treatment (Figure 10a and b). Followed by lepidopteran, Ag_2SNPs showed 100% mortality at 150 and 200 $\mu g{\cdot}ml^{-1}$ on *Ae. aegypti* after 40 and 48 h post-treatment (Figure 10c), whereas in *Cx. quinquefasciatus* Ag_2SNPs produced 100% mortality at 100, 150, and 200 $\mu g{\cdot}ml^{-1}$ after 36, 40, and 48 h treatment (Figure 10d). Similarly, in support of our research, Jafir et al. [16] found that the silver nanoparticles from *Ocimum basilicum* had effective insecticidal activity against *S. litura* at a dose of 1,500 $mg{\cdot}l^{-1}$. Further, the *Annona glabra*-derived NPs displayed potent larvicidal activity against the dengue vector *Ae. aegypti* and *Aedes albopictus* [44]. The essential oil-wrapped AgNPs showed good toxicity against the larvae and pupae of *Ae. albopictus* [45]. *Cassia hirsute*-derived AgNPs showed LC_{50} 4.43 ppm against *Cx. quinquefasciatus* [46]. Consequently, the results of this work bring up a new application for Ag_2SNPs from actinobacterial strain M10A62 and can be used as an alternative technique for pest management.

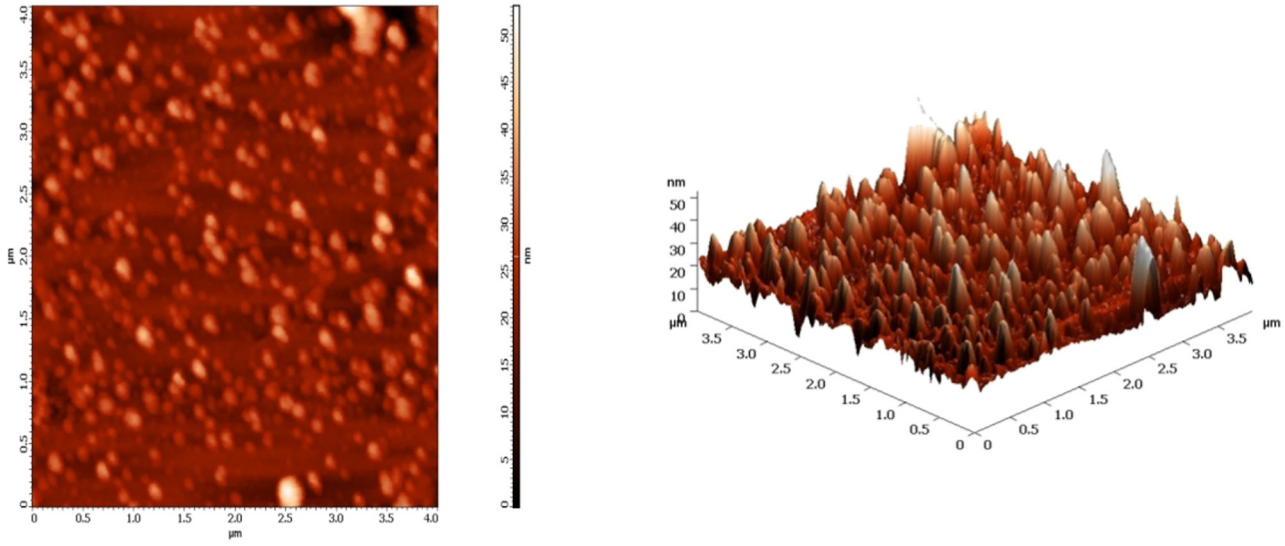

Figure 5: AFM images of *S. minutiscleroticus* derived Ag_2SNPs.

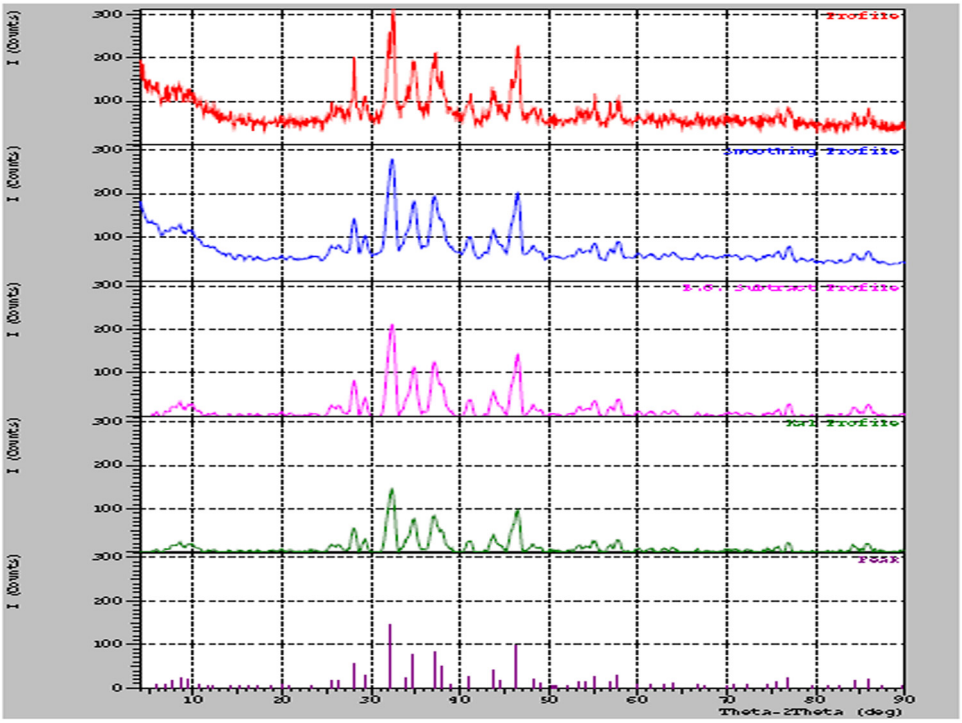

Figure 7: XRD pattern of *S. minutiscleroticus* derived Ag_2SNPs.

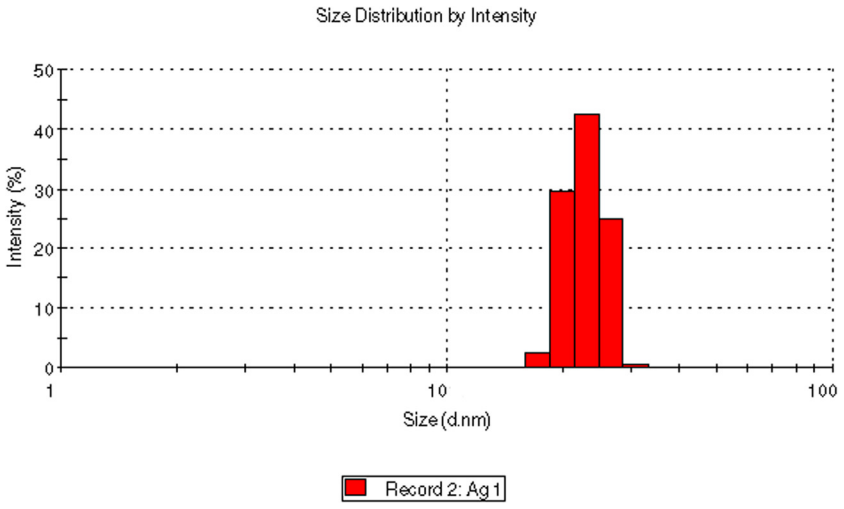

Figure 8: DLS of *S. minutiscleroticus* derived Ag_2SNPs.

4 Conclusion

In this research, an eco-friendly and target-specific stable Ag_2SNPs were fabricated from actinobacterial strain M10A62. The synthesized nanoparticles were confirmed by various bio-physical techniques, and the obtained nanoparticles were mostly spherical in shape with an average size ranging from 50 to 85 nm. Based on the results of this research, the Ag_2SNPs had significant toxicity on both crop and human pests. Overall, the actinobacterial-derived nanoparticles could be used as alternative insecticides in pest management programs since they are more affordable and safer. The process of biogenic synthesis may be optimized in the future, and field applications may be developed.

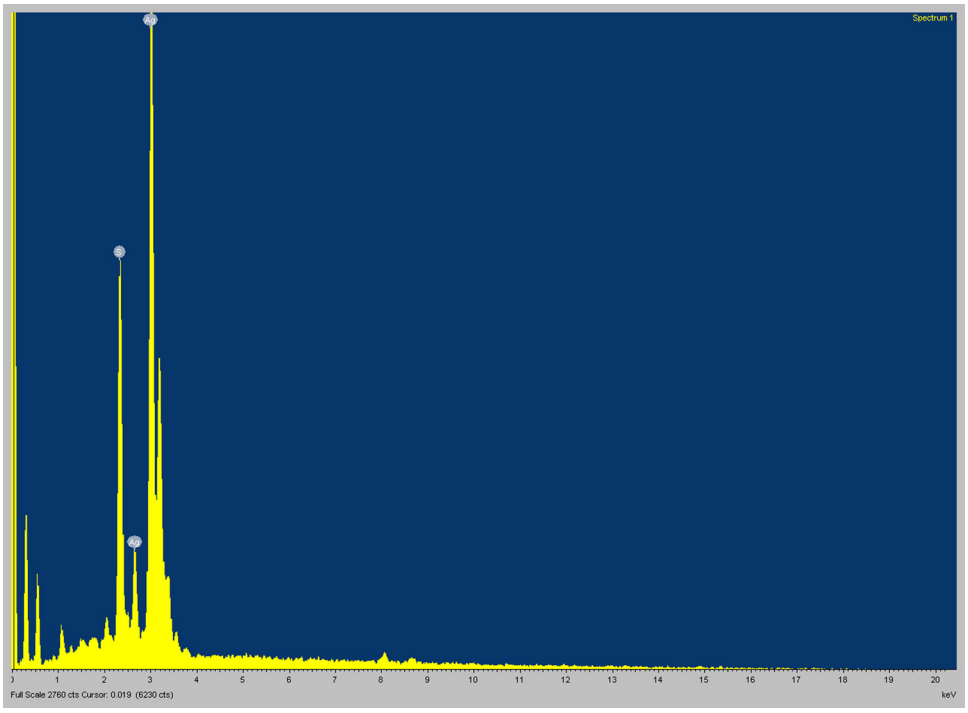

Figure 9: EDAX spectrum of *S. minutiscleroticus* derived Ag_2SNPs.

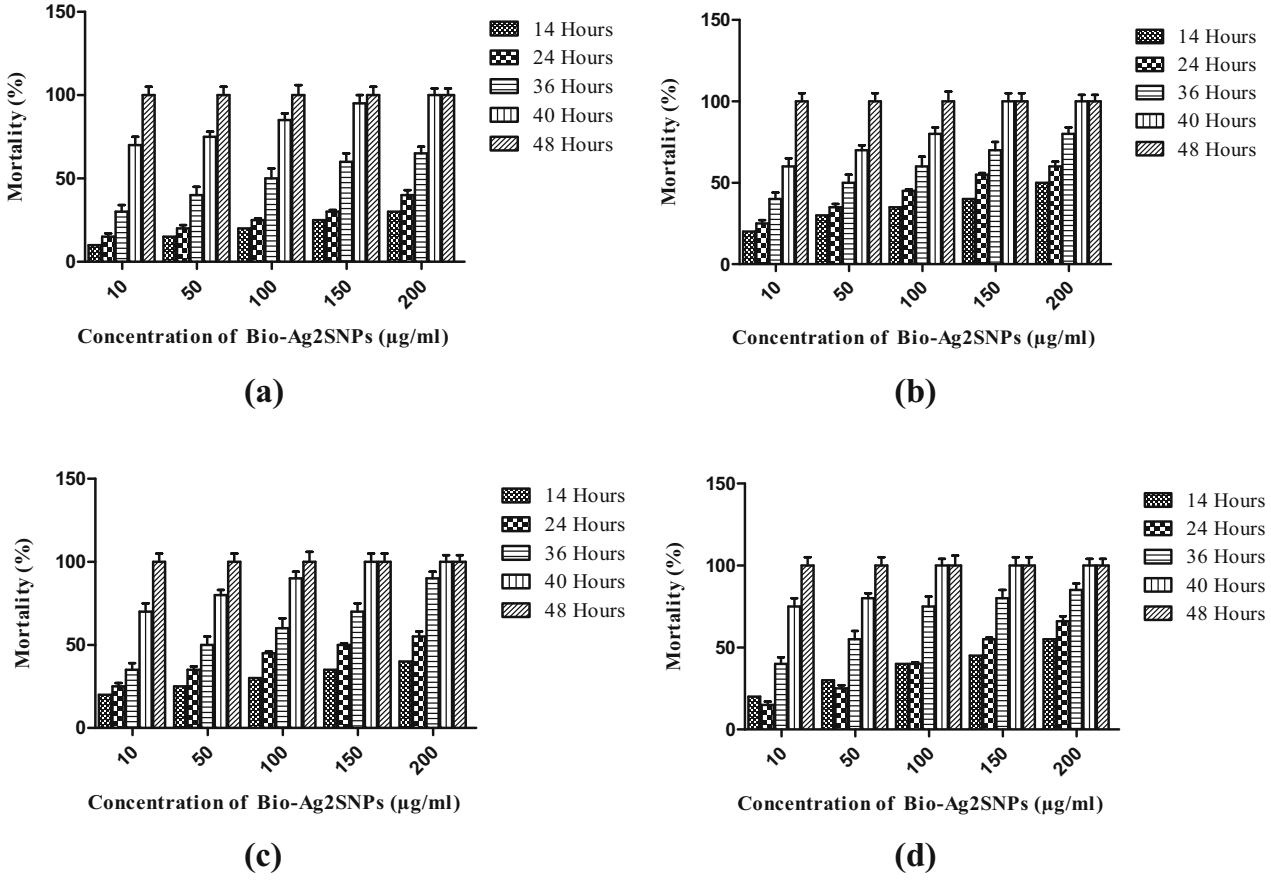

Figure 10: Insecticidal activity of Ag_2SNPs at different time intervals. (a) Insecticidal activity against *S. litura*. (b) *H. armigera*. (c) *Ae. aegypti*. (d) *Cx. quinquefasciatus*; Mortality (%) represents mean of three replicates, bar indicates standard deviation (SD) of the mean.

Funding information: Authors state no funding involved.

Conflict of interest: Authors state no conflict of interest.

Data availability statement: The datasets generated during and/or analyzed during the current study are available from the corresponding author on reasonable request.

References

[1] Sánchez-López E, Gomes D, Esteruelas G, Bonilla L, Lopez-Machado AL, Galindo R, et al. Metal-based nanoparticles as antimicrobial agents: an overview. Nanomaterials. 2020;10(2):292.

[2] Subramaniam S, Kumarasamy S, Narayanan M, Ranganathan M, Rathinavel T, Chinnathambi A, et al. Spectral and structure characterization of *Ferula assafoetida* fabricated silver nanoparticles and evaluation of its cytotoxic, and photocatalytic competence. Environ Res. 2022;204:111987.

[3] Ali SS, Moawad MS, Hussein MA, Azab M, Abdelkarim EA, Badr A, et al. Efficacy of metal oxide nanoparticles as novel antimicrobial agents against multi-drug and multi-virulent *Staphylococcus aureus* isolates from retail raw chicken meat and giblets. Int J Food Microbiol. 2021;344:109116.

[4] Ortigosa MS, Valenstein JS, Lin VSY, Trewyn BG, Wang K. Gold functionalized mesoporous silica nanoparticle mediated protein and DNA co delivery to plant cells via the biolistic method. Adv Funct Mater. 2012;22:3576–82.

[5] Benelli G. Mode of action of nanoparticles against insects. Environ Sci Pollut Res. 2018;25:12329–41.

[6] Kim B, Park CS, Murayama M, Hochella MF. Discovery and characterization of silver sulfide nanoparticles in final sewage sludge products. Environ Sci Technol. 2010;44(19):7509–14.

[7] Habeeb Rahuman HB, Dhandapani R, Narayanan S, Palanivel V, Paramasivam R, Subbarayalu R, et al. Medicinal plants mediated the green synthesis of silver nanoparticles and their biomedical applications. IET Nanobiotechnol. 2022;16(4):115–44.

[8] Manimaran M, Kannabiran K. Actinomycetes-mediated biogenic synthesis of metal and metal oxide nanoparticles: progress and challenges. Lett Appl Microbiol. 2017;64:401–8.

[9] Manivasagan P, Venkatesan J, Senthikumar K, Sivakumar K, Kim SK. Biosynthesis, antimicrobial and cytotoxic effect of silver nanoparticles using a novel *Nocardiopsis* sp. MBRC-1. Biomed Res Int. 2013;2013:287638.

[10] Wypij M, Czarnecka J, Swiecimska M, Dahm H, Rai M, Golinska P. Synthesis, characterization and evaluation of antimicrobial and cytotoxic activities of biogenic silver nanoparticles synthesized from *Streptomyces xinghaiensis* OF1 strain. World J Microbiol Biotechnol. 2018;34:1–13.

[11] Liao C, Li Y, Tjong SC. Bactericidal and cytotoxic properties of silver nanoparticles. Inter J Mol Sci. 2019;20:449.

[12] Zhang Z, Gao B, Qu C, Gong J, Li W, Luo C, et al. Resistance monitoring for six insecticides in vegetable field-collected populations of *Spodoptera litura* from China. Horticulturae. 2022;8(3):255.

[13] Muthusamy R, Shivakumar MS. Involvement of metabolic resistance and F1534C kdr mutation in the pyrethroid resistance mechanisms of *Aedes aegypti* in India. Acta Trop. 2015;148:137–41.

[14] Narayanan M, Ranganathan M, Subramanian SM, Kumarasamy S, Kandasamy S. Toxicity of cypermethrin and enzyme inhibitor synergists in red hairy caterpillar *Amsacta albistriga* (Lepidoptera: Arctiidae). J Basic Appl Zool. 2020;81:45.

[15] Narayanan M, Kumarasamy S, Ranganathan M, Kandasamy S, Kandasamy G, Gnanavel G. Enzyme and metabolites attained in degradation of chemical pesticides ß Cypermethrin by *Bacillus cereus*. Mater Today. 2020;33(7):3640–5.

[16] Jafir M, Ahmad JN, Arif MJ, Ali S, Ahmad SJN. Characterization of *Ocimum basilicum* synthesized silver nanoparticles and its relative toxicity to some insecticides against tobacco cutworm. Spodoptera litura Feb (Lepidoptera; Noctuidae) Ecotoxicol Environ Saf. 2021;218:112278.

[17] Pang M, Hu J, Zeng HC. Synthesis, morphological control, and antibacterial properties of hollow/solid Ag2S/Ag heterodimers. J Am Chem Soc. 2010;132:10771–85.

[18] Wang L, Hu C, Shao L. The antimicrobial activity of nanoparticles: present situation and prospects for the future. Int J Nanomed. 2017;12:1227–49.

[19] Ramya S, Shanmugasundaram T, Balagurunathan R. Biomedical potential of actinobacterially synthesized selenium nanoparticles with special reference to anti-biofilm, anti-oxidant, wound healing, cytotoxic and anti-viral activities. J Trace Elem Med Biol. 2015;32:30–9.

[20] Ramya S, Shanmugasundaram T, Balagurunathan R. Actinobacterial enzyme mediated synthesis of selenium nanoparticles for antibacterial, mosquito larvicidal and anthelminthic applications. Part Sci Technol. 2020;38(1):63–72.

[21] El Karkouri A, Assou SA, El Hassouni M. Isolation and screening of actinomycetes producing antimicrobial substances from an extreme Moroccan biotope. Pan Afr Med J. 2019;33:329.

[22] Vahabi K, Mansoori GA, Karimi S. Biosynthesis of silver nanoparticles by fungus *Trichoderma reesei* (a route for large-scale production of AgNPs). Sciences J. 2012;1(1):65–79.

[23] Khalil MA, El-Shanshoury AERR, Alghamdi MA, Alsalmi FA, Mohamed SF, Sun J, et al. Biosynthesis of silver nanoparticles by marine actinobacterium *Nocardiopsis dassonvillei* and exploring their therapeutic potentials. Front Microbiol. 2022;3(12):705673.

[24] Christensen L, Vivekanandhan S, Misra M, Mohanty AK. Biosynthesis of silver nanoparticles using Murraya koenigii (curry leaf): an investigation on the effect of broth concentration in reduction mechanism and particle size. Adv Mater Lett. 2011;2:429–34.

[25] Mohanty S, Mishra S, Jena P, Jacob B, Sarkar B, Sonawane A. An investigation on the antibacterial, cytotoxic, and antibiofilm efficacy of starch-stabilized silver nanoparticles. Nanomed Nanotechnol Biol Med. 2012;8(6):916–24.

[26] Mukherjee P, Ahmad A, Mandal D, Senapati S, Sainkar SR, Khan MI, et al. Fungus-mediated synthesis of silver nanoparticles and their immobilization in the mycelial matrix: a novel biological approach to nanoparticle synthesis. Nano Lett. 2001;1(10):515–9.

[27] Mohammed Fayaz A, Balaji K, Girilal M, Kalaichelvan PT, Venkatesan R. Mycobased synthesis of silver nanoparticles and their incorporation into sodium alginate films for vegetable and fruit preservation. J Agric Food Chem. 2009;57(14):6246–52.

[28] Smiechowicz E, Kulpinski P, Niekraszewicz B, Bacciarelli A. Cellulose fibers modified with silver nanoparticles. Cellulose. 2011;18:975–85.

[29] Goel N, Ahmad R, Singh R, Sood S, Khare S. Biologically synthesized silver nanoparticles by *Streptomyces* sp. EMB24 extracts used against the drug-resistant bacteria. Bioresour Technol Rep. 2021;15:100753.

[30] Bhattacharyya A, Prasad R, Buhroo AA, Duraisamy P, Yousuf I, Umadevi M, et al. One-pot fabrication and characterization of silver nanoparticles using *Solanum lycopersicum*: an eco-friendly and potent control tool against rose aphid, *Macrosiphum rosae*. J Nanosci. 2016;2016:4679410.
[31] Muthusamy R, Shivakumar MS. Susceptibility status of *Aedes aegypti* (L.) (Diptera: Culicidae) to temephos from three districts of Tamil Nadu, India. J Vector Borne Dis. 2015;52(2):159–65.
[32] Ganesan P, Reegan AD, David RHA, Gandhi MR, Paulraj MG, Al-Dhabi NA, et al. Antimicrobial activity of some actinomycetes from Western Ghats of Tamil Nadu, India. Alex Med J. 2017;53:101–10.
[33] Veerasamy R. Biosynthesis of silver nanoparticles using mangosteen leaf extract and evaluation of their antimicrobial activities. J Saudi Chem Soc. 2011;15:113–20.
[34] Awwad AM, Salem NM, Aqarbeh MM, Abdulaziz FM. Green synthesis, characterization of silver sulfide nanoparticles and antibacterial activity evaluation. Chem Int. 2000;6(1):42–8.
[35] Seyedeh MG, Sepideh H, Shojaosadati SA. Green synthesis of silver nanoparticles by a novel method: comparative study of their properties. Carbohydr Polym. 2012;89:467–72.
[36] Nazeruddin GM, Prasad SR, Shaikh YI, Ansari J, Sonawane KD, Nayak AK, et al. In-vitro bio-fabrication of multi-applicative silver nanoparticles using *Nicotiana tabacum* leaf extract. Life Sci Inf Public. 2016;2:6–30.
[37] Bharani RA, Namasivayam SKR. Biogenic silver nanoparticles mediated stress on developmental period and gut physiology of major lepidopteran pest *Spodoptera litura* (Fab.) (Lepidoptera: Noctuidae). An eco-friendly approach of insect pest control. J Environ Chem Eng. 2027;5:453–67.
[38] Das A, Mukherjee P, Singla SK, Guturu P, Frost MC, Mukhopadhyay D, et al. Fabrication and characterization of an inorganic gold and silica nanoparticle mediated drug delivery system for nitric oxide. Nanotechnology. 2010;21:305102.
[39] Siddiqi KS, Husen A, Rao RA. A review on biosynthesis of silver nanoparticles and their biocidal properties. J Nanobiotechnol. 2018;16:1–28.
[40] Hernández-Díaz JA, Garza-García JJ, León-Morales JM, Zamudio-Ojeda A, Arratia-Quijada J, Velázquez-Juárez G, et al. Antibacterial activity of biosynthesized selenium nanoparticles using extracts of *Calendula officinalis* against potentially clinical bacterial strains. Molecules. 2021;26(19):5929.
[41] Abdelsattar AS, Hakim TA, Rezk N, Farouk WM, Hassan YY, Gouda SM, et al. Green synthesis of silver nanoparticles using *Ocimum basilicum* L. and *Hibiscus sabdariffa* L. extracts and their antibacterial activity in combination with phage ZCSE6 and sensing properties. J Inorg Organomet Polym. 2022;32:1951–65.
[42] Ramkumar G, Asokan R, Ramya S, Gayathri G. Characterization of *Trigonella foenum-graecum* derived iron nanoparticles and its potential pesticidal activity against *Tuta absoluta* (Lepidoptera). J Clust Sci. 2021;32(1):1–6.
[43] Ramkumar G, Shivakumar MS, Alshehri MA, Panneerselvam C, Sayed SM. Larvicidal potential of *Cipadessa baccifera* leaf extract-synthesized zinc nanoparticles against three major mosquito vectors. Green Process Synth. 2022;11(1):757–65.
[44] Amarasinghe LD, Wickramarachchi PASR, Aberathna AAAU, Sithara WS, De Silva CR. Comparative study on larvicidal activity of green synthesized silver nanoparticles and *Annona glabra* (Annonaceae) aqueous extract to control *Aedes aegypti* and *Aedes albopictus* (Diptera: Culicidae). Heliyon. 2020;6(6):e04322. doi: 10.1016/j.heliyon.2020.e04322.
[45] Ga'al H, Fouad H, Mao G, Tian J, Jianchu M. Larvicidal and pupicidal evaluation of silver nanoparticles synthesized using *Aquilaria sinensis* and *Pogostemon cablin* essential oils against dengue and zika viruses vector Aedes albopictus mosquito and its histopathological analysis. Artif Cells Nanomed Biotechnol. 2018;46(6):1171–9.
[46] Adesuji ET, Oluwaniyi OO, Adegoke HI, Moodley R, Labulo AH, Bodede OS, et al. Investigation of the larvicidal potential of silver nanoparticles against *Culex quinquefasciatus*: a case of a ubiquitous weed as a useful bioresource. J Nanomater. 2016:1–11. doi: 10.1155/2016/4363751.